

First simultaneous measurement of Ξ^0 and $\bar{\Xi}^0$ asymmetry parameters in $\psi(3686)$ decay

M. Ablikim¹, M. N. Achasov^{13,b}, P. Adlarson⁷³, R. Aliberti³⁴, A. Amoroso^{72A,72C}, M. R. An³⁸, Q. An^{69,56}, Y. Bai⁵⁵, O. Bakina³⁵, I. Balossino^{29A}, Y. Ban^{45,g}, V. Batozskaya^{1,43}, K. Begzsuren³¹, N. Berger³⁴, M. Bertani^{28A}, D. Bettoni^{29A}, F. Bianchi^{72A,72C}, E. Bianco^{72A,72C}, J. Bloms⁶⁶, A. Bortone^{72A,72C}, I. Boyko³⁵, R. A. Briere⁵, A. Brueggemann⁶⁶, H. Cai⁷⁴, X. Cai^{1,56}, A. Calcaterra^{28A}, G. F. Cao^{1,61}, N. Cao^{1,61}, S. A. Cetin^{60A}, J. F. Chang^{1,56}, T. T. Chang⁷⁵, W. L. Chang^{1,61}, G. R. Che⁴², G. Chelkov^{35,a}, C. Chen⁴², Chao Chen⁵³, G. Chen¹, H. S. Chen^{1,61}, M. L. Chen^{1,56,61}, S. J. Chen⁴¹, S. M. Chen⁵⁹, T. Chen^{1,61}, X. R. Chen^{30,61}, X. T. Chen^{1,61}, Y. B. Chen^{1,56}, Y. Q. Chen³³, Z. J. Chen^{25,h}, W. S. Cheng^{72C}, S. K. Choi^{10A}, X. Chu⁴², G. Cibinetto^{29A}, S. C. Coen⁴, F. Cossio^{72C}, J. J. Cui⁴⁸, H. L. Dai^{1,56}, J. P. Dai⁷⁷, A. Dbeyssi¹⁹, R. E. de Boer⁴, D. Dedovich³⁵, Z. Y. Deng¹, A. Denig³⁴, I. Denysenko³⁵, M. Destefanis^{72A,72C}, F. De Mori^{72A,72C}, B. Ding^{64,1}, X. X. Ding^{45,g}, Y. Ding³³, Y. Ding³⁹, J. Dong^{1,56}, L. Y. Dong^{1,61}, M. Y. Dong^{1,56,61}, X. Dong⁷⁴, S. X. Du⁷⁹, Z. H. Duan⁴¹, P. Egorov^{35,a}, Y. L. Fan⁷⁴, J. Fang^{1,56}, S. S. Fang^{1,61}, W. X. Fang¹, Y. Fang¹, R. Farinelli^{29A}, L. Fava^{72B,72C}, F. Feldbauer⁴, G. Felici^{28A}, C. Q. Feng^{69,56}, J. H. Feng⁵⁷, K. Fischer⁶⁷, M. Fritsch⁴, C. Fritsch⁶⁶, C. D. Fu¹, Y. W. Fu¹, H. Gao⁶¹, Y. N. Gao^{45,g}, Yang Gao^{69,56}, S. Garbolino^{72C}, I. Garzia^{29A,29B}, P. T. Ge⁷⁴, Z. W. Ge⁴¹, C. Geng⁵⁷, E. M. Gersabeck⁶⁵, A. Gilman⁶⁷, K. Goetzen¹⁴, L. Gong³⁹, W. X. Gong^{1,56}, W. Gradl³⁴, S. Gramigna^{29A,29B}, M. Greco^{72A,72C}, M. H. Gu^{1,56}, Y. T. Gu¹⁶, C. Y. Guan^{1,61}, Z. L. Guan²², A. Q. Guo^{30,61}, L. B. Guo⁴⁰, R. P. Guo⁴⁷, Y. P. Guo^{12,f}, A. Guskov^{35,a}, X. T. Hou^{1,61}, W. Y. Han³⁸, X. Q. Hao²⁰, F. A. Harris⁶³, K. K. He⁵³, K. L. He^{1,61}, F. H. Heinsius⁴, C. H. Heinz³⁴, Y. K. Heng^{1,56,61}, C. Herold⁵⁸, T. Holtmann⁴, P. C. Hong^{12,f}, G. Y. Hou^{1,61}, Y. R. Hou⁶¹, Z. L. Hou¹, H. M. Hu^{1,61}, J. F. Hu^{54,i}, T. Hu^{1,56,61}, Y. Hu¹, G. S. Huang^{69,56}, K. X. Huang⁵⁷, L. Q. Huang^{30,61}, X. T. Huang⁴⁸, Y. P. Huang¹, T. Hussain⁷¹, N. Hüskens^{27,34}, W. Imoehl²⁷, M. Irshad^{69,56}, J. Jackson²⁷, S. Jaeger⁴, S. Janchiv³¹, J. H. Jeong^{10A}, Q. Ji¹, Q. P. Ji²⁰, X. B. Ji^{1,61}, X. L. Ji^{1,56}, Y. Y. Ji⁴⁸, Z. K. Jia^{69,56}, P. C. Jiang^{45,g}, S. S. Jiang³⁸, T. J. Jiang¹⁷, X. S. Jiang^{1,56,61}, Y. Jiang⁶¹, J. B. Jiao⁴⁸, Z. Jiao²³, S. Jin⁴¹, Y. Jin⁶⁴, M. Q. Jing^{1,61}, T. Johansson⁷³, X. Kui¹, S. Kabana³², N. Kalantar-Nayestanaki⁶², X. L. Kang⁹, X. S. Kang³⁹, R. Kappert⁶², M. Kavatsyuk⁶², B. C. Ke⁷⁹, A. Khoukaz⁶⁶, R. Kiuchi¹, R. Kliemt¹⁴, L. Koch³⁶, O. B. Kolcu^{60A}, B. Kopf⁴, M. Kuessner⁴, A. Kupsc^{43,73}, W. Kühn³⁶, J. J. Lane⁶⁵, J. S. Lange³⁶, P. Larin¹⁹, A. Lavania²⁶, L. Lavezzi^{72A,72C}, T. T. Lei^{69,k}, Z. H. Lei^{69,56}, H. Leithoff³⁴, M. Lellmann³⁴, T. Lenz³⁴, C. Li⁴², C. Li⁴⁶, C. H. Li³⁸, Cheng Li^{69,56}, D. M. Li⁷⁹, F. Li^{1,56}, G. Li¹, H. Li^{69,56}, H. B. Li^{1,61}, H. J. Li²⁰, H. N. Li^{54,i}, Hui Li⁴², J. R. Li⁵⁹, J. S. Li⁵⁷, J. W. Li⁴⁸, Ke Li¹, L. J. Li^{1,61}, L. K. Li¹, Lei Li³, M. H. Li⁴², P. R. Li^{37,j,k}, S. X. Li¹², T. Li⁴⁸, W. D. Li^{1,61}, W. G. Li¹, X. H. Li^{69,56}, X. L. Li⁴⁸, Xiaoyu Li^{1,61}, Y. G. Li^{45,g}, Z. J. Li⁵⁷, Z. X. Li¹⁶, Z. Y. Li⁵⁷, C. Liang⁴¹, H. Liang^{69,56}, H. Liang^{1,61}, H. Liang³³, Y. F. Liang⁵², Y. T. Liang^{30,61}, G. R. Liao¹⁵, L. Z. Liao⁴⁸, J. Libby²⁶, A. Limphirat⁵⁸, D. X. Lin^{30,61}, T. Lin¹, B. J. Liu¹, B. X. Liu⁷⁴, C. Liu³³, C. X. Liu¹, D. Liu^{19,69}, F. H. Liu⁵¹, Fang Liu¹, Feng Liu⁶, G. M. Liu^{54,i}, H. Liu^{37,j,k}, H. B. Liu¹⁶, H. M. Liu^{1,61}, Huanhuan Liu¹, Huihui Liu²¹, J. B. Liu^{69,56}, J. L. Liu⁷⁰, J. Y. Liu^{1,61}, K. Liu¹, K. Y. Liu³⁹, Ke Liu²², L. Liu^{69,56}, L. C. Liu⁴², Lu Liu⁴², M. H. Liu^{12,f}, P. L. Liu¹, Q. Liu⁶¹, S. B. Liu^{69,56}, T. Liu^{12,f}, W. K. Liu⁴², W. M. Liu^{69,56}, X. Liu^{37,j,k}, Y. Liu^{37,j,k}, Y. B. Liu⁴², Z. A. Liu^{1,56,61}, Z. Q. Liu⁴⁸, X. C. Lou^{1,56,61}, F. X. Lu⁵⁷, H. J. Lu²³, J. G. Lu^{1,56}, X. L. Lu¹, Y. Lu⁷, Y. P. Lu^{1,56}, Z. H. Lu^{1,61}, C. L. Luo⁴⁰, M. X. Luo⁷⁸, T. Luo^{12,f}, X. L. Luo^{1,56}, X. R. Lyu⁶¹, Y. F. Lyu⁴², F. C. Ma³⁹, H. L. Ma¹, J. L. Ma^{1,61}, L. L. Ma⁴⁸, M. M. Ma^{1,61}, Q. M. Ma¹, R. Q. Ma^{1,61}, R. T. Ma⁶¹, X. Y. Ma^{1,56}, Y. Ma^{45,g}, F. E. Maas¹⁹, M. Maggiora^{72A,72C}, S. Maldaner⁴, S. Malde⁶⁷, A. Mangoni^{28B}, Y. J. Mao^{45,g}, Z. P. Mao¹, S. Marcello^{72A,72C}, Z. X. Meng⁶⁴, J. G. Messchendorp^{14,62}, G. Mezzadri^{29A}, H. Miao^{1,61}, T. J. Min⁴¹, R. E. Mitchell²⁷, X. H. Mo^{1,56,61}, N. Yu. Muchnoi^{13,b}, Y. Nefedov³⁵, F. Nerling^{19,d}, I. B. Nikolaev^{13,b}, Z. Ning^{1,56}, S. Nisar^{11,l}, Y. Niu⁴⁸, S. L. Olsen⁶¹, Q. Ouyang^{1,56,61}, S. Pacetti^{28B,28C}, X. Pan⁵³, Y. Pan⁵⁵, A. Pathak³³, Y. P. Pei^{69,56}, M. Pelizaeus⁴, H. P. Peng^{69,56}, K. Peters^{14,d}, J. L. Ping⁴⁰, R. G. Ping^{1,61}, S. Plura³⁴, S. Pogodin³⁵, V. Prasad³², F. Z. Qi¹, H. Qi^{69,56}, H. R. Qi⁵⁹, M. Qi⁴¹, T. Y. Qi^{12,f}, S. Qian^{1,56}, W. B. Qian⁶¹, C. F. Qiao⁶¹, J. J. Qin⁷⁰, L. Q. Qin¹⁵, X. P. Qin^{12,f}, X. S. Qin⁴⁸, Z. H. Qin^{1,56}, J. F. Qiu¹, S. Q. Qu⁵⁹, C. F. Redmer³⁴, K. J. Ren³⁸, A. Rivetti^{72C}, V. Rodin⁶², M. Rolo^{72C}, G. Rong^{1,61}, Ch. Rosner¹⁹, S. N. Ruan⁴², N. Salone⁴³, A. Sarantsev^{35,c}, Y. Schelhaas³⁴, K. Schoenning⁷³, M. Scodreggio^{29A,29B}, K. Y. Shan^{12,f}, W. Shan²⁴, X. Y. Shan^{69,56}, J. F. Shangguan⁵³, L. G. Shao^{1,61}, M. Shao^{69,56}, C. P. Shen^{12,f}, H. F. Shen^{1,61}, W. H. Shen⁶¹, X. Y. Shen^{1,61}, B. A. Shi⁶¹, H. C. Shi^{69,56}, J. L. Shi¹², J. Y. Shi¹, Q. Q. Shi⁵³, R. S. Shi^{1,61}, X. Shi^{1,56}, J. J. Song²⁰, T. Z. Song⁵⁷, W. M. Song^{33,1}, Y. J. Song¹², Y. X. Song^{45,g}, S. Sosio^{72A,72C}, S. Spataro^{72A,72C}, F. Stieler³⁴, Y. J. Su⁶¹, G. B. Sun⁷⁴, G. X. Sun¹, H. Sun⁶¹, H. K. Sun¹, J. F. Sun²⁰, K. Sun⁵⁹, L. Sun⁷⁴, S. S. Sun^{1,61}, T. Sun^{1,61}, W. Y. Sun³³, Y. Sun⁹, Y. J. Sun^{69,56}, Y. Z. Sun¹, Z. T. Sun⁴⁸, Y. X. Tan^{69,56}, C. J. Tang⁵², G. Y. Tang¹, J. Tang⁵⁷, Y. A. Tang⁷⁴, L. Y. Tao⁷⁰, Q. T. Tao^{25,h}, M. Tat⁶⁷, J. X. Teng^{69,56}, V. Thoren⁷³, W. H. Tian⁵⁷, W. H. Tian⁵⁰, Y. Tian^{30,61}, Z. F. Tian⁷⁴, I. Uman^{60B}, B. Wang¹, B. L. Wang⁶¹, Bo Wang^{69,56}, C. W. Wang⁴¹, D. Y. Wang^{45,g}, F. Wang⁷⁰, H. J. Wang^{37,j,k}, H. P. Wang^{1,61}, K. Wang^{1,56}, L. L. Wang¹, M. Wang⁴⁸, Meng Wang^{1,61}, S. Wang^{12,f}, S. Wang^{37,j,k}, T. Wang^{12,f}, T. J. Wang⁴², W. Wang⁷⁰, W. Wang⁵⁷, W. H. Wang⁷⁴, W. P. Wang^{69,56}

X. Wang^{45,g}, X. F. Wang^{37,j,k}, X. J. Wang³⁸, X. L. Wang^{12,f}, Y. Wang⁵⁹, Y. D. Wang⁴⁴, Y. F. Wang^{1,56,61}, Y. H. Wang⁴⁶, Y. N. Wang⁴⁴, Y. Q. Wang¹, Yaqian Wang^{18,1}, Yi Wang⁵⁹, Z. Wang^{1,56}, Z. L. Wang⁷⁰, Z. Y. Wang^{1,61}, Ziyi Wang⁶¹, D. Wei⁶⁸, D. H. Wei¹⁵, F. Weidner⁶⁶, S. P. Wen¹, C. W. Wenzel⁴, U. Wiedner⁴, G. Wilkinson⁶⁷, M. Wolke⁷³, L. Wollenberg⁴, C. Wu³⁸, J. F. Wu^{1,61}, L. H. Wu¹, L. J. Wu^{1,61}, X. Wu^{12,f}, X. H. Wu³³, Y. Wu⁶⁹, Y. J. Wu³⁰, Z. Wu^{1,56}, L. Xia^{69,56}, X. M. Xian³⁸, T. Xiang^{45,g}, D. Xiao^{37,j,k}, G. Y. Xiao⁴¹, H. Xiao^{12,f}, S. Y. Xiao¹, Y. L. Xiao^{12,f}, Z. J. Xiao⁴⁰, C. Xie⁴¹, X. H. Xie^{45,g}, Y. Xie⁴⁸, Y. G. Xie^{1,56}, Y. H. Xie⁶, Z. P. Xie^{69,56}, T. Y. Xing^{1,61}, C. F. Xu^{1,61}, C. J. Xu⁵⁷, G. F. Xu¹, H. Y. Xu⁶⁴, Q. J. Xu¹⁷, W. L. Xu⁶⁴, X. P. Xu⁵³, Y. C. Xu⁷⁶, Z. P. Xu⁴¹, F. Yan^{12,f}, L. Yan^{12,f}, W. B. Yan^{69,56}, W. C. Yan⁷⁹, X. Q. Yan¹, H. J. Yang^{49,e}, H. L. Yang³³, H. X. Yang¹, Tao Yang¹, Y. Yang^{12,f}, Y. F. Yang⁴², Y. X. Yang^{1,61}, Yifan Yang^{1,61}, Z. W. Yang^{37,j,k}, M. Ye^{1,56}, M. H. Ye⁸, J. H. Yin¹, Z. Y. You⁵⁷, B. X. Yu^{1,56,61}, C. X. Yu⁴², G. Yu^{1,61}, T. Yu⁷⁰, X. D. Yu^{45,g}, C. Z. Yuan^{1,61}, L. Yuan², S. C. Yuan¹, X. Q. Yuan¹, Y. Yuan^{1,61}, Z. Y. Yuan⁵⁷, C. X. Yue³⁸, A. A. Zafar⁷¹, F. R. Zeng⁴⁸, X. Zeng^{12,f}, Y. Zeng^{25,h}, Y. J. Zeng^{1,61}, X. Y. Zhai³³, Y. H. Zhan⁵⁷, A. Q. Zhang^{1,61}, B. L. Zhang^{1,61}, B. X. Zhang¹, D. H. Zhang⁴², G. Y. Zhang²⁰, H. Zhang⁶⁹, H. H. Zhang⁵⁷, H. H. Zhang³³, H. Q. Zhang^{1,56,61}, H. Y. Zhang^{1,56}, J. J. Zhang⁵⁰, J. L. Zhang⁷⁵, J. Q. Zhang⁴⁰, J. W. Zhang^{1,56,61}, J. X. Zhang^{37,j,k}, J. Y. Zhang¹, J. Z. Zhang^{1,61}, Jiawei Zhang^{1,61}, L. M. Zhang⁵⁹, L. Q. Zhang⁵⁷, Lei Zhang⁴¹, P. Zhang¹, Q. Y. Zhang^{38,79}, Shuihan Zhang^{1,61}, Shulei Zhang^{25,h}, X. D. Zhang⁴⁴, X. M. Zhang¹, X. Y. Zhang⁵³, X. Y. Zhang⁴⁸, Y. Zhang⁶⁷, Y. T. Zhang⁷⁹, Y. H. Zhang^{1,56}, Yan Zhang^{69,56}, Yao Zhang¹, Z. H. Zhang¹, Z. L. Zhang³³, Z. Y. Zhang⁷⁴, Z. Y. Zhang⁴², G. Zhao¹, J. Zhao³⁸, J. Y. Zhao^{1,61}, J. Z. Zhao^{1,56}, Lei Zhao^{69,56}, Ling Zhao¹, M. G. Zhao⁴², S. J. Zhao⁷⁹, Y. B. Zhao^{1,56}, Y. X. Zhao^{30,61}, Z. G. Zhao^{69,56}, A. Zhemchugov^{35,a}, B. Zheng⁷⁰, J. P. Zheng^{1,56}, W. J. Zheng^{1,61}, Y. H. Zheng⁶¹, B. Zhong⁴⁰, X. Zhong⁵⁷, H. Zhou⁴⁸, L. P. Zhou^{1,61}, X. Zhou⁷⁴, X. K. Zhou⁶, X. R. Zhou^{69,56}, X. Y. Zhou³⁸, Y. Z. Zhou^{12,f}, J. Zhu⁴², K. Zhu¹, K. J. Zhu^{1,56,61}, L. Zhu³³, L. X. Zhu⁶¹, S. H. Zhu⁶⁸, S. Q. Zhu⁴¹, T. J. Zhu^{12,f}, W. J. Zhu^{12,f}, Y. C. Zhu^{69,56}, Z. A. Zhu^{1,61}, J. H. Zou¹, J. Zu^{69,56}

(BESIII Collaboration)

¹ *Institute of High Energy Physics, Beijing 100049, People's Republic of China*

² *Beihang University, Beijing 100191, People's Republic of China*

³ *Beijing Institute of Petrochemical Technology, Beijing 102617, People's Republic of China*

⁴ *Bochum Ruhr-University, D-44780 Bochum, Germany*

⁵ *Carnegie Mellon University, Pittsburgh, Pennsylvania 15213, USA*

⁶ *Central China Normal University, Wuhan 430079, People's Republic of China*

⁷ *Central South University, Changsha 410083, People's Republic of China*

⁸ *China Center of Advanced Science and Technology, Beijing 100190, People's Republic of China*

⁹ *China University of Geosciences, Wuhan 430074, People's Republic of China*

¹⁰ *Chung-Ang University, Seoul, 06974, Republic of Korea*

¹¹ *COMSATS University Islamabad, Lahore Campus, Defence Road, Off Raiwind Road, 54000 Lahore, Pakistan*

¹² *Fudan University, Shanghai 200433, People's Republic of China*

¹³ *G.I. Budker Institute of Nuclear Physics SB RAS (BINP), Novosibirsk 630090, Russia*

¹⁴ *GSI Helmholtzcentre for Heavy Ion Research GmbH, D-64291 Darmstadt, Germany*

¹⁵ *Guangxi Normal University, Guilin 541004, People's Republic of China*

¹⁶ *Guangxi University, Nanning 530004, People's Republic of China*

¹⁷ *Hangzhou Normal University, Hangzhou 310036, People's Republic of China*

¹⁸ *Hebei University, Baoding 071002, People's Republic of China*

¹⁹ *Helmholtz Institute Mainz, Staudinger Weg 18, D-55099 Mainz, Germany*

²⁰ *Henan Normal University, Xinxiang 453007, People's Republic of China*

²¹ *Henan University of Science and Technology, Luoyang 471003, People's Republic of China*

²² *Henan University of Technology, Zhengzhou 450001, People's Republic of China*

²³ *Huangshan College, Huangshan 245000, People's Republic of China*

²⁴ *Hunan Normal University, Changsha 410081, People's Republic of China*

²⁵ *Hunan University, Changsha 410082, People's Republic of China*

²⁶ *Indian Institute of Technology Madras, Chennai 600036, India*

²⁷ *Indiana University, Bloomington, Indiana 47405, USA*

²⁸ *INFN Laboratori Nazionali di Frascati, (A)INFN Laboratori Nazionali di Frascati, I-00044, Frascati, Italy; (B)INFN Sezione di Perugia, I-06100, Perugia, Italy; (C)University of Perugia, I-06100, Perugia, Italy*

²⁹ *INFN Sezione di Ferrara, (A)INFN Sezione di Ferrara, I-44122,*

- Ferrara, Italy; (B)University of Ferrara, I-44122, Ferrara, Italy
- ³⁰ Institute of Modern Physics, Lanzhou 730000, People's Republic of China
- ³¹ Institute of Physics and Technology, Peace Avenue 54B, Ulaanbaatar 13330, Mongolia
- ³² Instituto de Alta Investigación, Universidad de Tarapacá, Casilla 7D, Arica, Chile
- ³³ Jilin University, Changchun 130012, People's Republic of China
- ³⁴ Johannes Gutenberg University of Mainz, Johann-Joachim-Becher-Weg 45, D-55099 Mainz, Germany
- ³⁵ Joint Institute for Nuclear Research, 141980 Dubna, Moscow region, Russia
- ³⁶ Justus-Liebig-Universitaet Giessen, II. Physikalisches Institut, Heinrich-Buff-Ring 16, D-35392 Giessen, Germany
- ³⁷ Lanzhou University, Lanzhou 730000, People's Republic of China
- ³⁸ Liaoning Normal University, Dalian 116029, People's Republic of China
- ³⁹ Liaoning University, Shenyang 110036, People's Republic of China
- ⁴⁰ Nanjing Normal University, Nanjing 210023, People's Republic of China
- ⁴¹ Nanjing University, Nanjing 210093, People's Republic of China
- ⁴² Nankai University, Tianjin 300071, People's Republic of China
- ⁴³ National Centre for Nuclear Research, Warsaw 02-093, Poland
- ⁴⁴ North China Electric Power University, Beijing 102206, People's Republic of China
- ⁴⁵ Peking University, Beijing 100871, People's Republic of China
- ⁴⁶ Qufu Normal University, Qufu 273165, People's Republic of China
- ⁴⁷ Shandong Normal University, Jinan 250014, People's Republic of China
- ⁴⁸ Shandong University, Jinan 250100, People's Republic of China
- ⁴⁹ Shanghai Jiao Tong University, Shanghai 200240, People's Republic of China
- ⁵⁰ Shanxi Normal University, Linfen 041004, People's Republic of China
- ⁵¹ Shanxi University, Taiyuan 030006, People's Republic of China
- ⁵² Sichuan University, Chengdu 610064, People's Republic of China
- ⁵³ Soochow University, Suzhou 215006, People's Republic of China
- ⁵⁴ South China Normal University, Guangzhou 510006, People's Republic of China
- ⁵⁵ Southeast University, Nanjing 211100, People's Republic of China
- ⁵⁶ State Key Laboratory of Particle Detection and Electronics, Beijing 100049, Hefei 230026, People's Republic of China
- ⁵⁷ Sun Yat-Sen University, Guangzhou 510275, People's Republic of China
- ⁵⁸ Suranaree University of Technology, University Avenue 111, Nakhon Ratchasima 30000, Thailand
- ⁵⁹ Tsinghua University, Beijing 100084, People's Republic of China
- ⁶⁰ Turkish Accelerator Center Particle Factory Group, (A)Istinye University, 34010, Istanbul, Turkey; (B)Near East University, Nicosia, North Cyprus, 99138, Mersin 10, Turkey
- ⁶¹ University of Chinese Academy of Sciences, Beijing 100049, People's Republic of China
- ⁶² University of Groningen, NL-9747 AA Groningen, The Netherlands
- ⁶³ University of Hawaii, Honolulu, Hawaii 96822, USA
- ⁶⁴ University of Jinan, Jinan 250022, People's Republic of China
- ⁶⁵ University of Manchester, Oxford Road, Manchester, M13 9PL, United Kingdom
- ⁶⁶ University of Muenster, Wilhelm-Klemm-Strasse 9, 48149 Muenster, Germany
- ⁶⁷ University of Oxford, Keble Road, Oxford OX13RH, United Kingdom
- ⁶⁸ University of Science and Technology Liaoning, Anshan 114051, People's Republic of China
- ⁶⁹ University of Science and Technology of China, Hefei 230026, People's Republic of China
- ⁷⁰ University of South China, Hengyang 421001, People's Republic of China
- ⁷¹ University of the Punjab, Lahore-54590, Pakistan
- ⁷² University of Turin and INFN, (A)University of Turin, I-10125, Turin, Italy; (B)University of Eastern Piedmont, I-15121, Alessandria, Italy; (C)INFN, I-10125, Turin, Italy
- ⁷³ Uppsala University, Box 516, SE-75120 Uppsala, Sweden
- ⁷⁴ Wuhan University, Wuhan 430072, People's Republic of China
- ⁷⁵ Xinyang Normal University, Xinyang 464000, People's Republic of China
- ⁷⁶ Yantai University, Yantai 264005, People's Republic of China
- ⁷⁷ Yunnan University, Kunming 650500, People's Republic of China

⁷⁸ Zhejiang University, Hangzhou 310027, People's Republic of China

⁷⁹ Zhengzhou University, Zhengzhou 450001, People's Republic of China

^a Also at the Moscow Institute of Physics and Technology, Moscow 141700, Russia

^b Also at the Novosibirsk State University, Novosibirsk, 630090, Russia

^c Also at the NRC "Kurchatov Institute", PNPI, 188300, Gatchina, Russia

^d Also at Goethe University Frankfurt, 60323 Frankfurt am Main, Germany

^e Also at Key Laboratory for Particle Physics, Astrophysics and Cosmology, Ministry of Education; Shanghai Key Laboratory for Particle Physics and Cosmology; Institute of Nuclear and Particle Physics, Shanghai 200240, People's Republic of China

^f Also at Key Laboratory of Nuclear Physics and Ion-beam Application (MOE) and Institute of Modern Physics, Fudan University, Shanghai 200443, People's Republic of China

^g Also at State Key Laboratory of Nuclear Physics and Technology, Peking University, Beijing 100871, People's Republic of China

^h Also at School of Physics and Electronics, Hunan University, Changsha 410082, China

ⁱ Also at Guangdong Provincial Key Laboratory of Nuclear Science, Institute of Quantum Matter, South China Normal University, Guangzhou 510006, China

^j Also at Frontiers Science Center for Rare Isotopes, Lanzhou University, Lanzhou 730000, People's Republic of China

^k Also at Lanzhou Center for Theoretical Physics, Key Laboratory of Theoretical Physics of Gansu Province, and Key Laboratory for Quantum Theory and Applications of the MoE, Lanzhou University, Lanzhou 730000, People's Republic of China

^l Also at the Department of Mathematical Sciences, IBA, Karachi, Pakistan

(Dated: July 11, 2023)

The Ξ^0 asymmetry parameters are measured using entangled quantum $\Xi^0\bar{\Xi}^0$ pairs from a sample of $(448.1 \pm 2.9) \times 10^6$ $\psi(3686)$ events collected with the BESIII detector at BEPCII. The relative phase between the transition amplitudes of the $\Xi^0\bar{\Xi}^0$ helicity states is measured to be $\Delta\Phi = -0.050 \pm 0.150 \pm 0.020$ rad, which implies that there is no obvious polarization at the current level of statistics. The decay parameters of the Ξ^0 hyperon (α_{Ξ^0} , $\alpha_{\bar{\Xi}^0}$, ϕ_{Ξ^0} , $\phi_{\bar{\Xi}^0}$) and the angular distribution parameter ($\alpha_{\psi(3686)}$) and $\Delta\Phi$ are measured simultaneously for the first time. In addition, the CP asymmetry observables are determined to be $A_{CP}^{\Xi^0} = (\alpha_{\Xi^0} + \alpha_{\bar{\Xi}^0})/(\alpha_{\Xi^0} - \alpha_{\bar{\Xi}^0}) = -0.007 \pm 0.082 \pm 0.025$ and $\Delta\phi_{CP}^{\Xi^0} = (\phi_{\Xi^0} + \phi_{\bar{\Xi}^0})/2 = -0.079 \pm 0.082 \pm 0.010$ rad, which are consistent with CP conservation.

The universe began with the Big Bang, where it is commonly assumed that matter and antimatter were created in equal amounts. However, at present, only traces of antimatter can be seen. CP violation (CPV) is one of the necessary conditions to possibly explain this asymmetry [1]. The existence of CPV in the decays of K^0 , B^0 , and D^0 mesons [2–5], as well as in neutrino oscillations ν_l [6], are firmly established. However, these CPV effects are too small to explain the large matter-antimatter asymmetry in the universe.

Recently, a technique to test CPV in the hyperon sector has been developed by simultaneously analyzing the spin polarization and the asymmetry parameters of the entangled hyperon-antihyperon pairs produced in the decays of the J/ψ , $\psi(3686)$, and $\psi(3770)$ mesons at the BESIII experiment [7]. For cascade hyperon decays, the angular distribution of the daughter hyperon is proportional to $(1 + \alpha_H \mathbf{P}_H \cdot \hat{\mathbf{n}})$, where α_H is the hyperon decay parameter, \mathbf{P}_H and $\hat{\mathbf{n}}$ are the hyperon polarization and the unit vector in the direction of the daughter hyperon momentum, respectively, both in the hyperon rest frame. The CP asymmetry is defined as $A_{CP} = (\alpha_H + \alpha_{\bar{H}})/(\alpha_H - \alpha_{\bar{H}})$, where the parameters α_H and $\alpha_{\bar{H}}$ are CP odd, and a nonzero A_{CP} indicates CPV. In the Standard Model (SM), a tiny A_{CP} value of $\sim 10^{-4}$ [8] is predicted in the hyperon sector. Therefore, a test of CPV in hyperon de-

cays is sensitive to possible sources of CPV from physics beyond the SM [9, 10]. At present, BESIII has performed CPV tests in the decays of Λ [11–13], Σ^+ [14], and Ξ^- [15, 16] hyperons, where for Ξ^- hyperons, the most precise asymmetry parameter measurement was reported in J/ψ decay. BESIII has also performed the first determination of the weak phase of the Ξ^- hyperon using entangled $\Xi^-\bar{\Xi}^+$ pairs [15]. However, CPV in Ξ^0 hyperon decays has not so far been searched for, the asymmetry parameter α_{Ξ^0} in the decay $\Xi^0 \rightarrow \Lambda\pi^0$ has not been measured directly, only the product $\alpha_{\Lambda} \cdot \alpha_{\Xi^0}$ has been reported [17, 18], and the weak decay phase ϕ_{Ξ^0} was measured with large uncertainty [19–21].

The process of $e^+e^- \rightarrow \psi(3686) \rightarrow \Xi^0\bar{\Xi}^0 \rightarrow \pi^0\pi^0\Lambda\bar{\Lambda}$ with $\Lambda \rightarrow p\pi^-$ can be fully described by the vector $\boldsymbol{\xi} = (\theta_{\Xi}, \theta_{\Lambda}, \varphi_{\Lambda}, \theta_{\bar{\Lambda}}, \varphi_{\bar{\Lambda}}, \theta_p, \varphi_p, \theta_{\bar{p}}, \varphi_{\bar{p}})$, where the coordinate systems and angles are shown in Fig. ?? with the same convention as Refs. [15] and [16]. The cascade Ξ and Λ polarization vector, \mathbf{P}_{Ξ} and \mathbf{P}_{Λ} , are related as $\mathbf{P}_{\Lambda} = \alpha_{\Xi^0}\hat{\mathbf{z}}_{\Xi^0} + \beta_{\Xi^0}(\mathbf{P}_{\Xi^0} \times \hat{\mathbf{z}}_{\Xi^0}) + \gamma_{\Xi^0}[\hat{\mathbf{z}}_{\Xi^0} \times (\mathbf{P}_{\Xi^0} \times \hat{\mathbf{z}}_{\Xi^0})]$, where α_{Ξ^0} , β_{Ξ^0} , and γ_{Ξ^0} are defined in Ref. [22] and $\hat{\mathbf{z}}_{\Xi^0}$ is the unit vector in the direction of the Ξ momentum. The joint angular distribution function is described by [23]

$$\begin{aligned} \mathcal{W} &= \mathcal{W}(\xi, \Omega) \\ &= \sum_{\mu, \bar{\nu}=0}^3 \sum_{\mu'=0}^3 \sum_{\bar{\nu}'=0}^3 C_{\mu\bar{\nu}} a_{\mu\mu'}^{\Xi} a_{\mu'\bar{\nu}'}^{\Lambda} a_{\bar{\nu}\bar{\nu}'}^{\Xi} a_{\bar{\nu}'0}^{\bar{\Lambda}}, \end{aligned} \quad (1)$$

where $C_{\mu\nu}$ is the production spin density matrix, $a_{\mu\nu}$ is the joint decay amplitude, and $\Omega = (\alpha_{\psi(3686)}, \Delta\Phi, \alpha_{\Xi^0}, \phi_{\Xi^0}, \alpha_{\Lambda}, \alpha_{\bar{\Lambda}}, \alpha_{\Xi^0}, \phi_{\Xi^0})$ is the set of decay parameters. The definitions of $C_{\mu\nu}$ and $a_{\mu\nu}$ may be found in Ref. [23].

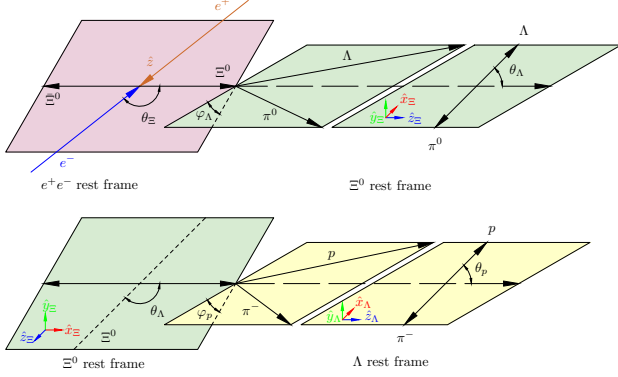


FIG. 1. Depiction of the axes orientation used in the analysis of the Ξ^0 decay parameters. In the e^+e^- rest frame, the \hat{z} axis is along the e^+ direction, and \hat{z}_{Ξ^0} is along the Ξ^0 momentum direction. In the Ξ^0 rest frame, the polar axis direction is \hat{z}_{Ξ^0} , \hat{y}_{Ξ^0} is along $\hat{z} \times \hat{z}_{\Xi^0}$ and \hat{z}_{Λ} is along the Λ momentum direction. For the Λ rest frame, the polar axis direction is \hat{z}_{Λ} and \hat{y}_{Λ} is along $\hat{z}_{\Xi^0} \times \hat{z}_{\Lambda}$. The vector $\hat{P}_{\Xi^0} \times \hat{z}_{\Lambda}$ is along the \hat{y}_{Λ} axis. The definition for the $\bar{\Xi}^0$ is analogous, with the $\hat{z}_{\bar{\Xi}^0}$ axis against the \hat{z}_{Ξ^0} direction.

CPV is searched for with an amplitude, A_{CP} , and a phase, $\Delta\phi_{CP}$, defined as

$$\begin{aligned} A_{CP}^{\Xi^0} &= \frac{\alpha_{\Xi^0} + \alpha_{\bar{\Xi}^0}}{\alpha_{\Xi^0} - \alpha_{\bar{\Xi}^0}}, \\ \Delta\phi_{CP}^{\Xi^0} &= \frac{1}{2} (\phi_{\Xi^0} + \phi_{\bar{\Xi}^0}). \end{aligned} \quad (2)$$

The polarization observable P_y is defined as follows [24],

$$P_y = \frac{\sqrt{1 - \alpha_{\psi(3686)}^2} \sin 2\theta_{\Xi} \sin \Delta\Phi}{2(1 + \alpha_{\psi(3686)} \cos^2 \theta_{\Xi})}, \quad (3)$$

which is dependent on the transverse polarization parameter $\Delta\Phi$.

In this paper, we present the first simultaneous measurement of the Ξ^0 asymmetry parameters using entangled Ξ^0 - $\bar{\Xi}^0$ pairs from $(448.1 \pm 2.9) \times 10^6$ $\psi(3686)$ decays [25] collected with the BESIII detector [26]. In addition, a study of the transverse polarization in $\psi(3686) \rightarrow \Xi^0 \bar{\Xi}^0$ and a test of CPV in Ξ^0 hyperon decays are performed.

Candidate $\psi(3686) \rightarrow \Xi^0 \bar{\Xi}^0$ events are selected by fully reconstructing the subsequent decays $\Xi^0 \rightarrow \pi^0 \Lambda$, $\Lambda \rightarrow p \pi^-$ and $\pi^0 \rightarrow \gamma\gamma$ (as well as the charge conjugate final states for $\bar{\Xi}$ and $\bar{\Lambda}$ decays). Potential background contributions are studied with an inclusive Monte Carlo (MC) simulation sample of $\psi(3686)$ decays [27], and an exclusive simulation of the signal process with 5×10^6 events is generated with a phase space model for normalization. The production of the $\psi(3686)$ resonance for both MC samples is simulated with the KKMC generator [28, 29], and the subsequent decays are processed by EVTGEN [30, 31]. Additionally for the inclusive MC sample, the branching fractions of cascade decays are fixed according to the Particle Data Group (PDG) [32]. All the remaining unmeasured decay modes are generated with LUNDCHARM [33, 34]. The response of the BESIII detector is modeled with MC simulations using a framework based on GEANT4 [35, 36].

Candidate events are required to contain at least four charged particles (two positive and two negative) and at least four photons. Charged particles are reconstructed as tracks within the multilayer drift chamber (MDC). Only tracks fully contained in the acceptance region of the MDC, $|\cos \theta| < 0.93$ (with θ defined with respect to the z -axis, which is the symmetry axis of the MDC), are kept for the analysis. Because of the momentum separation in the two body decay, the momenta of (anti-)proton and charged pion candidates are required to be greater and less than $0.5 \text{ GeV}/c$, respectively.

$\Lambda(\bar{\Lambda})$ candidates are reconstructed as $p\pi^-(\bar{p}\pi^+)$ pairs that satisfy a vertex fit. The four-track combination that minimizes $\sqrt{(M_{p\pi^-} - m_{\Lambda})^2 + (M_{\bar{p}\pi^+} - m_{\Lambda})^2}$ is selected, where $M_{p\pi^-}$ ($M_{\bar{p}\pi^+}$) is the invariant mass of the $p\pi^-$ ($\bar{p}\pi^+$) pair and m_{Λ} is the Λ mass from the PDG [32]. To further suppress non- Λ background, the Λ decay length is required to be greater than zero, where negative decay lengths are caused by the detector resolution and background contributions.

Photon candidates are reconstructed from isolated showers in the electromagnetic calorimeter (EMC). The energy deposited in the nearby time of flight (TOF) counter is included to improve the reconstruction efficiency and energy resolution. The shower energies are required to be greater than 25 MeV in the EMC barrel region ($|\cos \theta| < 0.8$), or greater than 50 MeV in the EMC end-cap region ($0.86 < |\cos \theta| < 0.92$). In order to reject electronic noise and energy deposits unrelated to the event start time, the EMC shower time, measured with respect to the collision signal, is required to satisfy $0 < t < 700 \text{ ns}$.

To further suppress background from soft π^0 s and radiated photon events and to improve the mass resolution, a six-constraint (6C) kinematic fit is applied to all possible $\gamma\gamma\gamma\gamma\Lambda\bar{\Lambda}$ combinations by imposing energy-momentum conservation and constraining the masses of the two pairs of photons from the π^0 mesons to the π^0 mass. The Ξ^0 and $\bar{\Xi}^0$ candidates are then reconstructed as the $\pi^0\Lambda$ and $\pi^0\bar{\Lambda}$ combinations that minimize the discriminant $\delta =$

$\sqrt{(M_{\pi^0\Lambda} - m_{\Xi^0})^2 + (M_{\pi^0\bar{\Lambda}} - m_{\Xi^0})^2}$ from all $\pi^0\Lambda(\pi^0\bar{\Lambda})$ combinations, where $M_{\pi^0\Lambda}(M_{\pi^0\bar{\Lambda}})$ is the invariant mass of the $\pi^0\Lambda(\pi^0\bar{\Lambda})$ system and m_{Ξ^0} is the Ξ^0 mass from the PDG [32]. Finally, background contributions from the $\psi(3686) \rightarrow \pi^0\pi^0 J/\psi$ process are rejected by requiring the recoil mass of $\pi^0\pi^0$ combinations to be at least 20 MeV/c^2 away from the nominal J/ψ mass [32]. Figure ?? shows the distribution of $M_{\pi^0\Lambda}$ versus $M_{\pi^0\bar{\Lambda}}$ for candidate events selected in data. A clear signal around the $\Xi^0(\bar{\Xi}^0)$ mass is observed. Signal events are required to simultaneously satisfy $|M_{\pi^0\Lambda} - m_{\Xi^0}| < 15 \text{ MeV}/c^2$ and $|M_{\pi^0\bar{\Lambda}} - m_{\Xi^0}| < 15 \text{ MeV}/c^2$ (region marked as S in Fig. ??). Most of the background contributions arise from $\psi(3686)$ decays that do not contain a $\Xi^0\bar{\Xi}^0$ pair, such as $\psi(3686) \rightarrow \pi^0\pi^0\Lambda\bar{\Lambda}$. The background yield is evaluated by the mean of the three sideband regions B_i (with $i = 1, 2, 3$) depicted in Fig. ?. The sideband regions have the same size as the signal region, but are centered on the following values of $(M_{\pi^0\Lambda}, M_{\pi^0\bar{\Lambda}}) = (1.27, 1.27)$, $(1.36, 1.27)$, and $(1.27, 1.36)$ GeV/c^2 . The sideband region B_4 is not suitable for background evaluation as it is close to the $\psi(3686) \rightarrow \Sigma(1385)^0\bar{\Sigma}(1385)^0$ region and would lead to an overestimation of the signal contamination. In the signal region $N = 1934$ events are counted with an expected background contribution of 23 ± 5 events, resulting in a 1.2% contamination level. The signal contamination can, therefore, be considered as negligible in the following analysis.

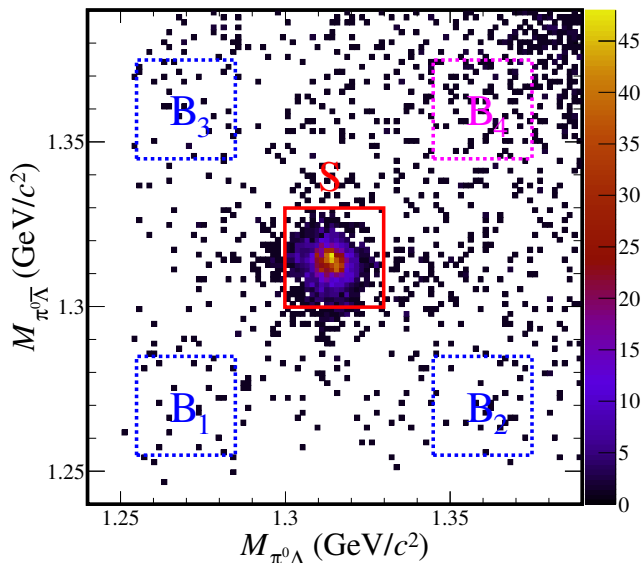


FIG. 2. The scatter plot of $M_{\pi^0\Lambda}$ versus $M_{\pi^0\bar{\Lambda}}$ of the candidate events selected from data, where the red box S shows the signal region, the blue boxes B_1 , B_2 , and B_3 denote the selected sideband regions, and the magenta box B_4 is close to the $\Sigma(1385)^0\bar{\Sigma}(1385)^0$ signal and is not used.

To determine the set of Ω parameters, an unbinned maximum likelihood fit (MLL fit) is performed, where the decay parameters α_Λ and $\alpha_{\bar{\Lambda}}$ are fixed to 0.754 [11] assuming CP conservation in Λ and $\bar{\Lambda}$ decays. In the fit, the likelihood func-

tion \mathcal{L} is given by

$$\mathcal{L} = \prod_{i=1}^N \frac{\mathcal{W}(\xi_i, \Omega)\epsilon(\xi_i)}{\mathcal{N}(\Omega)}, \quad (4)$$

where the joint angular distribution \mathcal{W} is defined in Eq. (1), N is the number of data events, $\epsilon = N_{\text{survive}}^{\text{MC}}/N_{\text{total}}^{\text{MC}}$ is the detection efficiency, and $\mathcal{N}(\Omega) = \int \mathcal{W}(\xi_i, \Omega)\epsilon(\xi_i)d\xi_i$ is the normalization factor. Since the low background level has a negligible effect, we do not include a background term in the fit, and the parameters are determined by minimizing the function $S = -\ln \mathcal{L}$. The fit results are reported in Table I.

TABLE I. Numerical results of parameters, where the first uncertainty is statistical and the second is systematic.

Param.	This work	BESIII [38]	PDG [32]
$\alpha_{\psi(3686)}$	$0.665 \pm 0.086 \pm 0.081$	$0.650 \pm 0.090 \pm 0.140$...
$\Delta\Phi$	$-0.050 \pm 0.150 \pm 0.020$
α_{Ξ^0}	$-0.358 \pm 0.042 \pm 0.013$...	-0.356 ± 0.011
ϕ_{Ξ^0}	$0.027 \pm 0.117 \pm 0.011$...	0.366 ± 0.209
$\alpha_{\bar{\Xi}^0}$	$0.363 \pm 0.042 \pm 0.013$
$\phi_{\bar{\Xi}^0}$	$-0.185 \pm 0.116 \pm 0.017$
A_{CP}^{Ξ}	$-0.007 \pm 0.082 \pm 0.025$
$\Delta\phi_{CP}^{\Xi}$	$-0.079 \pm 0.082 \pm 0.010$...	-

Systematic uncertainties arise from the difference of detection efficiencies between data and simulations (tracking, π^0 and $\Xi^0(\bar{\Xi}^0)$ reconstruction, 6C kinematic fit, $\pi^0\pi^0 J/\psi$ background veto) as well as from the sideband technique, background from the continuum process $e^+e^- \rightarrow \Xi^0\bar{\Xi}^0$, the uncertainties of the $\Lambda \rightarrow p\pi^-$ decay parameters and the MLL fit method as listed in Table II. Correction factors for tracking and π^0 reconstruction efficiency differences between data and simulations are evaluated on a control sample of $\psi(3686) \rightarrow \Xi^0\bar{\Xi}^0$ events, where one of the hyperon is fully reconstructed and one of the charged particles (p, \bar{p}, π^+ and π^-) or the π^0 from the second is not considered. The uncertainties arising from the correction procedure are evaluated by mean of 100 variation of the correction factors, following a Gaussian distribution with the nominal value as mean and the statistical uncertainty as width. The difference between the nominal results of the decay parameters and the mean values of those obtained through the variations is regarded as systematic uncertainty. The correction to the Ξ^0 reconstruction efficiency differences is evaluated as in Ref. [37–45], and the same procedure is applied to estimate the systematic uncertainty. The 6C kinematic fit is sensitive to differences in the momentum resolution of the charged tracks between data and simulations. Corrections to the helix parameters of charged tracks are evaluated and applied in the measurement, and the difference between the spin polarization parameters obtained with and without the corrections is considered as the systematic uncertainty. The systematic uncertainty from vetoing $\psi(3686) \rightarrow \pi^0\pi^0 J/\psi$ background is estimated by varying the range of the mass window requirement by 5 MeV/c^2 . The largest difference is taken as the uncertainty. The uncertainties related to background contributions (sideband evaluation and continuum process) are

evaluated by introducing a background term to the MLL function $S \rightarrow S' = -\ln \mathcal{L} + \ln \mathcal{L}_{\text{BKG}}$. The difference in the fit results is taken as the uncertainty. The possible bias introduced by the $\Lambda \rightarrow p\pi^-$ decay parameters are estimated by changing a_Λ and $a_{\bar{\Lambda}}$ values reported in Ref. [11] by $\pm 1\sigma$. The largest variation with respect to the central value is considered as the systematic uncertainty. To validate the fit procedures, an input-output check based on 300 pseudo-experiments is performed with the helicity amplitude formula Eq. (1). The polarization and the asymmetry decay parameters measured in this analysis are used as input in the formula. The number of events in each generated MC sample is 5000, and the check is performed independently 300 times. The difference between the input and output Gaussian fit values is taken as the systematic uncertainty caused by the fit method. Assuming all sources to be independent, the total systematic uncertainties in the measurement of α_{Ξ^0} , $\Delta\Phi$ and the decay asymmetry parameters via analyzing for $\psi(3686) \rightarrow \Xi^0\Xi^0$ are determined as the sum in quadrature of the mentioned sources.

TABLE II. Systematic uncertainties of the measured parameters.

Source	$\alpha_{\psi(3686)}$	$\Delta\Phi$	α_{Ξ^0}	ϕ_{Ξ^0}	α_{Ξ^0}	ϕ_{Ξ^0}
Tracking efficiency	0.067	0.003	0.003	0.004	0.002	0.004
π^0 reconstruction	0.032	0.001	0.001	0.002	0.001	0.000
Ξ^0 reconstruction	0.024	0.003	0.001	0.001	0.000	0.001
6C kinematic fit	0.006	0.003	0.001	0.001	0.000	0.001
$\pi^0\pi^0 J/\psi$ background veto	0.016	0.017	0.009	0.004	0.007	0.013
Sideband subtraction	0.011	0.000	0.004	0.006	0.002	0.002
Continuum process	0.011	0.000	0.004	0.006	0.002	0.003
Λ decay parameter	0.001	0.006	0.006	0.004	0.005	0.000
Fit method	0.008	0.009	0.003	0.002	0.008	0.010
Total	0.081	0.020	0.013	0.011	0.013	0.017

In summary, based on a data sample of $(448.1 \pm 2.9) \times 10^6$ $\psi(3686)$ events collected with the BESIII detector, the Ξ^0 asymmetry parameters are measured with high precision using entangled quantum $\Xi^0\Xi^0$ pairs. The numerical results are summarized in Table I. The polarization signal related with Eq. (3) is shown in Fig. 3. The value of $\alpha_{\psi(3686)}$ is measured to be $0.665 \pm 0.086 \pm 0.081$, which is consistent with the previous BESIII measurement [38], and $\Delta\Phi = -0.050 \pm 0.150 \pm 0.020$ rad is measured for the first time and is significantly different from the one for Ξ^- reported in Refs. [15, 16]. The relative phase that is approximately zero implies an insignificant transverse polarization, which differs from the polarization observed in Λ decays from J/ψ decays, Σ^+ decays from both J/ψ and $\psi(3686)$ decays, and Ξ^- decays from both J/ψ and $\psi(3686)$ decays [11, 14–16]. The asymmetry parameters α_{Ξ} and α_{Ξ} are determined simultaneously for the first time. Previously only the product of $\alpha_\Lambda \cdot \alpha_{\Xi^0}$ [17, 18] was reported. The parameter ϕ_{Ξ^0} is measured more precisely compared with the value reported by the HBC group almost half a century ago [19–21]. In addition, the Ξ^0 hyperon CP asymmetry parameters $A_{CP}^{\Xi^0}$, $\Delta\phi_{CP}^{\Xi^0}$, as summarized in Table I, indicate no CPV effect at the current level of accuracy. It is expected that the test of CPV will reach sensitivities comparable to the SM prediction when a

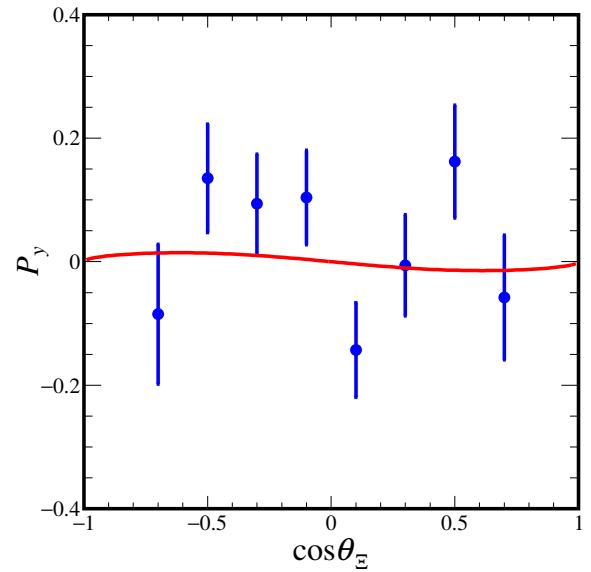


FIG. 3. Distribution of the polarization observable P_y versus $\cos\theta_{\Xi}$, dots with error bars represent experimental data, and the red line denotes the global fit result.

large data sample will be available at BESIII [46], the upcoming PANDA experiment at FAIR [47], and the proposed Super Tau-Charm Factory projects in China and Russia [48, 49].

The BESIII Collaboration thanks the staff of BEPCII and the IHEP computing center for their strong support. This work is supported in part by National Key R&D Program of China under Contracts Nos. 2020YFA0406400, 2020YFA0406300; National Natural Science Foundation of China (NSFC) under Contracts Nos. 12075107, 12247101, 11635010, 11735014, 11835012, 11905236, 11935015, 11935016, 11935018, 11961141012, 12022510, 12025502, 12035009, 12035013, 12047501, 12061131003, 12192260, 12192261, 12192262, 12192263, 12192264, 12192265, 12225509; the Chinese Academy of Sciences (CAS) Large-Scale Scientific Facility Program; the CAS Center for Excellence in Particle Physics (CCEPP); Joint Large-Scale Scientific Facility Funds of the NSFC and CAS under Contract No. U1832207; CAS Key Research Program of Frontier Sciences under Contracts Nos. QYZDJ-SSW-SLH003, QYZDJ-SSW-SLH040; 100 Talents Program of CAS; The Institute of Nuclear and Particle Physics (INPAC) and Shanghai Key Laboratory for Particle Physics and Cosmology; ERC under Contract No. 758462; European Union’s Horizon 2020 research and innovation programme under Marie Skłodowska-Curie grant agreement under Contract No. 894790; German Research Foundation DFG under Contracts Nos. 443159800, 455635585, Collaborative Research Center CRC 1044, FOR5327, GRK 2149; Istituto Nazionale di Fisica Nucleare, Italy; Ministry of Development of Turkey under Contract No. DPT2006K-120470; National Research Foundation of Korea under Contract No. NRF-2022R1A2C1092335; National Science and Technology fund; National Science Research and Innovation Fund

(NSRF) via the Program Management Unit for Human Resources & Institutional Development, Research and Innovation under Contract No. B16F640076; Polish National Science Centre under Contract No. 2019/35/O/ST2/02907; Suranaree University of Technology (SUT), Thailand Science Research and Innovation (TSRI), and National Science Research and Innovation Fund (NSRF) under Contract No. 160355; The Royal Society, UK under Contract No. DH160214; The Swedish Research Council; U. S. Department of Energy under Contract No. DE-FG02-05ER41374.

-
- [1] A. D. Sakharov, *Psi'ma Zh. Eksp. Teor. Fiz.* **5**, 32 (1967).
 [2] J. H. Christenson, J. W. Cronin, V. L. Fitch, and R. Turlay, *Phys. Rev. Lett.* **13**, 138 (1964).
 [3] B. Aubert *et al.* (BABAR Collaboration), *Phys. Rev. Lett.* **87**, 091801 (2001).
 [4] K. Abe *et al.* (Belle Collaboration), *Phys. Rev. Lett.* **87**, 091802 (2001).
 [5] R. Aaij *et al.* (LHCb Collaboration), *Phys. Rev. Lett.* **122**, 211803 (2019).
 [6] K. Abe *et al.* (T2K Collaboration), *Nature* **580**, 339 (2020).
 [7] X. G. He, J. Tandean and G. Valencia, *Sci. Bull.* **67**, 1840 (2022).
 [8] J. F. Donoghue, X. G. He and S. Pakvasa, *Phys. Rev. D* **34**, 833 (1986).
 [9] D. G. Ireland, M. Döring, D. I. Glazier, J. Haidenbauer, M. Mai, R. Murray-Smith and D. Rönchen, *Phys. Rev. Lett.* **123**, 182301 (2019).
 [10] H. Liu, J. Zhang and X. Wang, *Symmetry* **15**, 214 (2023).
 [11] M. Ablikim *et al.* (BESIII Collaboration), *Nature Phys.* **15**, 631 (2019).
 [12] M. Ablikim *et al.* (BESIII Collaboration), *Phys. Rev. D* **105**, L011101 (2022).
 [13] M. Ablikim *et al.* (BESIII Collaboration), *Phys. Rev. Lett.* **129**, 131801 (2022).
 [14] M. Ablikim *et al.* (BESIII Collaboration), *Phys. Rev. Lett.* **125**, 052004 (2020).
 [15] M. Ablikim *et al.* (BESIII Collaboration), *Nature* **606**, 64 (2022).
 [16] M. Ablikim *et al.* (BESIII Collaboration), *Phys. Rev. D* **106**, L091101 (2022).
 [17] R. Handler *et al.*, *Phys. Rev. D* **25**, 639 (1982).
 [18] J. R. Batley *et al.* (NA48/1 Collaboration), *Phys. Lett. B* **693**, 241 (2010).
 [19] J. P. Berge, P. Eberhard, J. R. Hubbard, D. W. Merrill, J. Button-Shafer, F. T. Solmitz and M. L. Stevenson, *Phys. Rev.* **147**, 945 (1966).
 [20] P. M. Dauber, J. P. Berge, J. R. Hubbard, D. W. Merrill and R. A. Muller, *Phys. Rev.* **179** 1262 (1969).
 [21] C. Baltay, A. Bridgewater, W. A. Cooper, L. K. Gershwin, M. Habibi, M. Kalelkar, N. Yeh and A. Gaigalas, *Phys. Rev. D* **9**, 49 (1974).
 [22] T. D. Lee and C. N. Yang, *Phys. Rev.* **108** 1645 (1957).
 [23] E. Perotti, G. Fäldt, A. Kupsc, S. Leupold and J. J. Song, *Phys. Rev. D* **99**, 056008 (2019).
 [24] G. Fäldt and A. Kupsc, *Phys. Lett. B* **772**, 16 (2017).
 [25] M. Ablikim *et al.* (BESIII Collaboration), *Chin. Phys. C* **42**, 023001 (2018).
 [26] M. Ablikim *et al.* (BESIII Collaboration), *Nucl. Instrum. Meth. A* **614**, 345 (2010).
 [27] X. Zhou, S. Du, G. Li and C. Shen, *Comput. Phys. Commun.* **258**, 107540 (2021).
 [28] S. Jadach, B. F. L. Ward and Z. Was, *Comput. Phys. Commun.* **130**, 260 (2000).
 [29] S. Jadach, B. F. L. Ward and Z. Was, *Phys. Rev. D* **63**, 113009 (2001).
 [30] D. J. Lange, *Nucl. Instrum. Meth. A* **462**, 152 (2001).
 [31] R. G. Ping, *Chin. Phys. C* **32**, 599 (2008).
 [32] R. L. Workma *et al.* (Particle Data Group), *Prog. Theor. Exp. Phys.* **2022**, 083C01 (2022).
 [33] J. C. Chen, G. S. Huang, X. R. Qi, D. H. Zhang and Y. S. Zhu, *Phys. Rev. D* **62**, 034003 (2000).
 [34] R. L. Yang, R. G. Ping and H. Chen, *Chin. Phys. Lett.* **31**, 061301 (2014).
 [35] S. Agostinelli *et al.* (GEANT4 Collaboration), *Nucl. Instrum. Meth. A* **506**, 250 (2003).
 [36] J. Allison *et al.*, *IEEE Trans. Nucl. Sci.* **53**, 270 (2006).
 [37] M. Ablikim *et al.* (BESIII Collaboration), *Phys. Rev. D* **93**, 072003 (2016).
 [38] M. Ablikim *et al.* (BESIII Collaboration), *Phys. Lett. B* **770**, 217 (2017).
 [39] M. Ablikim *et al.* (BESIII Collaboration), *Phys. Rev. D* **100**, 051101 (2019).
 [40] M. Ablikim *et al.* (BESIII Collaboration), *Phys. Rev. Lett.* **124**, 032002 (2020).
 [41] M. Ablikim *et al.* (BESIII Collaboration), *Phys. Rev. D* **103**, 012005 (2021).
 [42] M. Ablikim *et al.* (BESIII Collaboration), *Phys. Lett. B* **820**, 136557 (2021).
 [43] M. Ablikim *et al.* (BESIII Collaboration), *Phys. Rev. D* **104**, L091104 (2021).
 [44] M. Ablikim *et al.* (BESIII Collaboration), *Phys. Rev. D* **104**, 092012 (2021).
 [45] M. Ablikim *et al.* (BESIII Collaboration), *J. High Energy Phys.* **06** (2022) 74.
 [46] M. Ablikim *et al.* (BESIII Collaboration), *Chin. Phys. C* **44**, 040001 (2020).
 [47] W. Erni *et al.* (PANDA Collaboration), *arXiv* 0903.3905 (2009) [hep-ex].
 [48] A. E. Bondar *et al.* (Charm-Tau Factory Collaboration), *Phys. Atom. Nucl.* **76**, 1072 (2013).
 [49] X. D. Shi, X. R. Zhou, X. S. Qin and H. P. Peng, *J. Instrum.* **16**, P03029 (2021).